

Sympathetic control of bone mass regulated by osteopontin

Masashi Nagao^{a,b,c,1}, Timothy N. Feinstein^{d,1}, Yoichi Ezura^{a,c,e,f}, Tadayoshi Hayata^{a,c}, Takuya Notomi^{a,c}, Yoshitomo Saita^b, Ryo Hanyu^{a,b,c}, Hiroaki Hemmi^{a,c,g}, Yayoi Izu^a, Shu Takeda^c, Kathryn Wang^h, Susan Rittlingⁱ, Tetsuya Nakamoto^{a,c}, Kazuo Kaneko^b, Hisashi Kurosawa^b, Gerard Karsenty^j, David T. Denhardt^h, Jean-Pierre Vilardaga^{d,2}, and Masaki Noda^{a,c,e,f,g,2}

^aDepartment of Molecular Pharmacology, Medical Research Institute, and ^cGlobal Center of Excellence Program, International Research Center for Molecular Science in Tooth and Bone Diseases, Tokyo Medical and Dental University, 1-5-45 Yushima, Bunkyo-ku, 113-8510 Tokyo, Japan; ^bDepartment of Orthopedics, School of Medicine, Juntendo University, 2-1-1 Hongo, Bunkyo-ku, 113-8421 Tokyo, Japan; ^dMedical Top Track Program, Medical Research Institute, Tokyo Medical and Dental University, 1-5-45 Yushima, Bunkyo-ku, 113-8510 Tokyo, Japan; ^eDepartment of Cell Biology and Neuroscience, Rutgers, The State University of New Jersey, Piscataway, NJ 08701; ^fForsyth Institute, Boston, MA 02115; ^gDepartment of Genetics and Development, College of Physicians and Surgeons, Columbia University, New York, NY 10032; ^hAdvanced Bone and Joint Science Program, Tokyo Medical and Dental University, 1-5-45 Yushima, Bunkyo-ku, 113-8510 Tokyo, Japan; ⁱHard Tissue Genome Research Center, Tokyo Medical and Dental University, 1-5-45 Yushima, Bunkyo-ku, 113-8510 Tokyo, Japan; and ^jLaboratory for GPCR Biology, Department of Pharmacology and Chemical Biology, School of Medicine, University of Pittsburgh, Pittsburgh, PA 15261

Edited by Harvey Cantor, Dana-Farber Cancer Institute, Boston, MA, and approved September 8, 2011 (received for review June 13, 2011)

The sympathetic nervous system suppresses bone mass by mechanisms that remain incompletely elucidated. Using cell-based and murine genetics approaches, we show that this activity of the sympathetic nervous system requires osteopontin (OPN), a cytokine and one of the major members of the noncollagenous extracellular matrix proteins of bone. In this work, we found that the stimulation of the sympathetic tone by isoproterenol increased the level of OPN expression in the plasma and bone and that mice lacking OPN (OPN-KO) suppressed the isoproterenol-induced bone loss by preventing reduced osteoblastic and enhanced osteoclastic activities. In addition, we found that OPN is necessary for changes in the expression of genes related to bone resorption and bone formation that are induced by activation of the sympathetic tone. At the cellular level, we showed that intracellular OPN modulated the capacity of the β 2-adrenergic receptor to generate cAMP with a corresponding modulation of cAMP-response element binding (CREB) phosphorylation and associated transcriptional events inside the cell. Our results indicate that OPN plays a critical role in sympathetic tone regulation of bone mass and that this OPN regulation is taking place through modulation of the β 2-adrenergic receptor/cAMP signaling system.

osteoporosis | G protein-coupled receptor | osteoblast

Bone formation and bone resorption require a tight regulation of the two facets of bone metabolism: new bone deposition by osteoblasts and bone resorption by osteoclast cells. Pathologic bone loss and bone accumulation disorders are nearly always caused by dysregulation of this balance, either toward bone accumulation (e.g., osteopetrosis) or bone loss (e.g., osteopenia or osteoporosis). The most common disorder of bone loss, osteoporosis, contributes to a high fracture risk and challenges quality of life and longevity of affected populations such as the elderly and postmenopausal women (1). Osteoporosis can also develop after prolonged inactivity or weightless space travel because of the loss of mechanical stress stimuli that promote anabolic bone remodeling and inhibit resorption (2–4). Unlike bone loss from unloading and inactivity, postmenopausal osteoporosis is characterized by both an increase in bone formation as well as a relatively greater increase in bone resorption, and bone deterioration therefore proceeds more slowly. The primary regulators of bone metabolism include hormones such as parathyroid hormone (PTH) and parathyroid hormone-related protein (PTHrP), inflammatory and anti-inflammatory cytokines, and the sympathetic tone of the nervous system, which regulates bone mass through neurotransmitters such as epinephrine and norepinephrine via innervation of bone cells (5, 6). As in the case of disuse (unloading) osteoporosis, bone loss through the sympathetic tone is charac-

terized by stimulation of bone resorption and suppression of bone formation (7). Conversely, inhibition of the sympathetic tone by β -blockers suppresses unloading-induced bone loss by suppressing bone resorption and enhancing bone formation (8). Nonetheless, the mechanism by which the sympathetic tone regulates bone metabolism remains largely unknown.

Osteopontin (OPN), a major member of the noncollagenous extracellular matrix secreted by osteoblasts and a cytokine involved in proliferation, apoptosis, and inflammatory signaling, has been implicated in bone remodeling after mechanical stress (9). Indeed, OPN-deficient mice show both increased deposition and reduced resorption of bone after unloading (10–12). In terms of the control of bone metabolism, the OPN-KO phenotype therefore phenocopies treatment with β -blockers. Here, we hypothesize that OPN serves as a molecular link between the sympathetic tone and bone metabolism. Using a combination of mouse KO studies and cell-based assays, we find that intracellular OPN acts by modulating activity of the β 2-adrenergic receptor (β 2AR), a G protein-coupled receptor (GPCR) expressed in osteoblasts and involved in regulation of bone resorption in response to the activity of sympathetic nerves (7). This study thus suggests that intracellular OPN links bone to the sympathetic tone via regulation of the β 2AR signaling cascade.

Results

OPN is necessary for bone loss mediated by a sympathomimetic ligand. To determine whether the sympathetic nervous system influences expression of OPN, we measured the level of circulating OPN after injection of isoproterenol (ISO), a sympathomimetic ligand, or saline vehicle into the peritoneum of mice of two different strains. ISO treatment increased plasma OPN in both 129sv mice (Fig. 1A) and C57BL/6 mice (Fig. 1B). This increase originated, at least in part, from bone, where an increase in OPN mRNA expression was also detected in response to ISO (Fig. 1C).

Author contributions: M. Nagao, T.N.F., J.-P.V., and M. Noda designed research; M. Nagao, T.N.F., Y.E., T.H., T. Notomi, Y.S., R.H., H.H., Y.I., and J.-P.V. performed research; S.T., K.W., S.R., T. Nakamoto, K.K., H.K., G.K., and D.T.D. contributed new reagents/analytic tools; J.-P.V. and M. Noda analyzed data; and J.-P.V. and M. Noda wrote the paper.

The authors declare no conflict of interest.

This article is a PNAS Direct Submission.

¹M. Nagao and T.F. contributed equally to this work.

²To whom correspondence may be addressed. E-mail: noda.mph@mri.tmd.ac.jp or jpv@pitt.edu.

This article contains supporting information online at www.pnas.org/lookup/suppl/doi:10.1073/pnas.1109402108/-DCSupplemental.

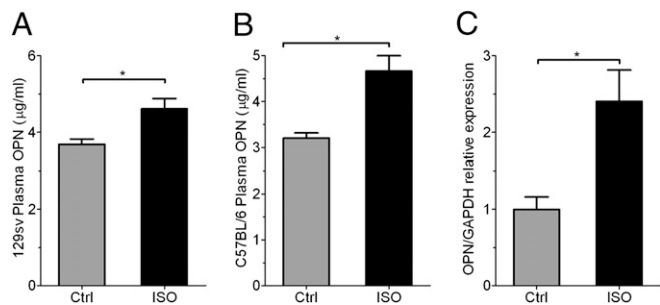


Fig. 1. ISO treatment up-regulates OPN levels in bone and circulation. (A and B) OPN protein expression in circulation for both 129sv (A) and C57BL/6 (B) mice in response to ISO treatment. ($n = 3-4$ per group, $*P < 0.05$.) (C) OPN mRNA expression in bone in vivo in response to ISO treatment, normalized to GAPDH mRNA expression. Results are in arbitrary units as mean \pm SEM of $n = 4$ ($*P < 0.05$).

We next examined bone structure and bone mass after injection of ISO into OPN-deficient (OPN-KO) and WT mice. Microcomputed tomography (μ CT) analyses of long bone showed a reduction in crowdedness of trabecular bone after ISO injection in WT mice (Fig. 2A vs. B) but not in OPN-KO mice (Fig. 2C vs. D). Quantification indicated that ISO significantly reduced bone mass [bone volume/tissue volume (BV/TV)] and

trabecular number in WT mice, whereas ISO injection into OPN-KO mice had no effect (Fig. 2E and G). ISO treatment also enhanced the levels of trabecular separation (Fig. 2F) and trabecular spacing (Fig. 2H) in WT but not in OPN-KO mice. This observation was not limited to long bone because similar effects were observed in vertebrae (Fig. 2I-L), where ISO significantly reduced BV/TV in WT but not in OPN-KO mice (Fig. 2M). As was the case with long bone, OPN deficiency also reduced the effect of ISO on structural parameters in vertebral bone such as trabecular number (Fig. 2O), trabecular separation (Fig. 2N), and trabecular spacing (Fig. 2P). Thus, OPN is necessary for ISO-induced bone loss in both vertebral and long bones. ISO treatment increased OPN expression in cultured bone, indicating that the catabolic effect of ISO on bone is most likely mediated by direct control of OPN expression (Fig. S1).

Sympathetic nervous tone requires OPN to increase osteoclast activity and to decrease osteoblast activity. We next examined whether OPN mediates ISO-induced bone resorption by increasing osteoclastic activity, decreasing osteoblast activity, or both. Administration of ISO in WT mice increased both histomorphometric and biochemical parameters of bone resorption, including the number of osteoclasts, the levels of bone surface covered by tartrate-resistant acid phosphatase-positive (TRAP⁺) cells (osteoclast surface per bone surface) (Fig. 3A-D), and urine levels of deoxypyridinoline, a marker of systemic bone destruction that reflects collagen degradation mediated by osteoclastic activity

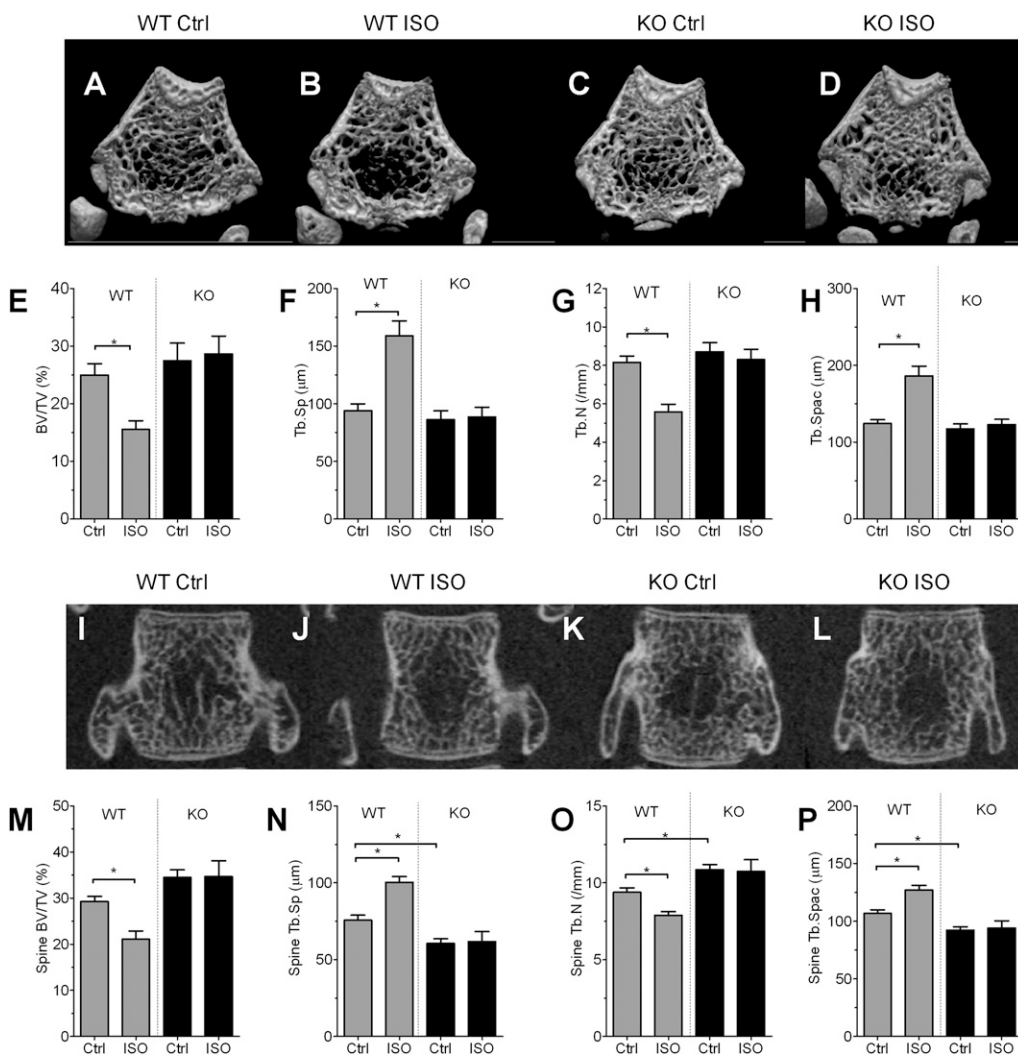


Fig. 2. OPN deficiency suppresses ISO-induced bone loss. (A-D) Representative 3D- μ CT images of the distal metaphyseal regions of femora in vehicle (A and C) and ISO treatment (B and D) groups of WT (A and B) and OPN-KO (C and D) mice. (E-H) Bone parameters measured from data shown in A-D. (E) BV/TV. (F) Trabecular separation (Tb.Sp). (G) Trabecular number (Tb.N). (H) Trabecular spacing (Tb.Spac). Data represent the mean \pm SEM of $n = 7-8$ mice per group ($*P < 0.05$). (I-L) Representative 2D- μ CT images of vertebrae in mice treated with vehicle (I and K) and ISO treatment (J and L) groups of WT (I and J) and OPN-KO (K and L) mice. (M-P) Bone parameters measured from data shown in I-L. (M) BV/TV. (N) Trabecular separation (Tb.Sp). (O) Trabecular number (Tb.N). (P) Trabecular spacing (Tb.Spac). Data represent the mean \pm SEM of $n = 7-8$ mice per group ($*P < 0.05$).

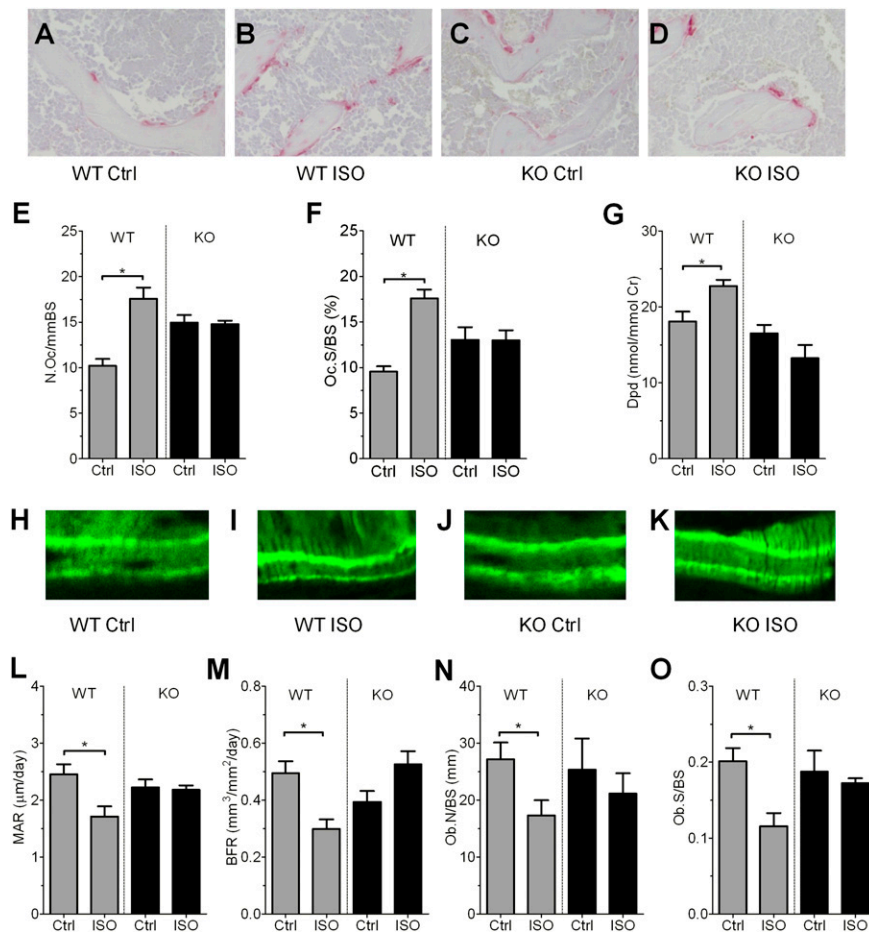


Fig. 3. OPN control of the inhibitory effect of ISO on bone remodeling. (A–D) Secondary trabecular regions of the epiphyses of tibiae were examined for osteoclasts based on TRAP staining in vehicle (A and C) and ISO treatment (B and D) groups of WT (A and B) and OPN-KO (C and D) mice. (E–G) Parameters of osteoclast activity. Number of osteoclasts per bone surface (N.Oc/BS) (E), osteoclast surface per bone surface (Oc.S/BS) (F), and urinary deoxyypyridinoline (Dpd) (G) excretion levels are shown. Bars represent the mean \pm SEM of $n = 5$ –9 mice per group ($*P < 0.05$). (H–K) Bone formation activity was evaluated in vivo as described in *Materials and Methods*. Calcein bands were visualized to obtain dynamic histomorphometric parameters. (L–O) Parameters of osteoblast activity. Levels of mineral apposition rate (MAR) (L), bone formation rate (BFR) (M), osteoblast number (Ob.N/BS) (N), and osteoblast surface (Ob.S/BS) (O) are shown. Bars represent the mean \pm SEM of $n = 5$ mice per group ($*P < 0.05$).

(Fig. 3 A, B, and E–G, gray bars). OPN deficiency suppressed the stimulatory effect of ISO on all parameters of bone resorption (Fig. 3 C–G, black bars). However, the slightly higher osteoclast number and osteoclast surfaces in OPN-KO compared with WT mice at baseline ($P < 0.01$) could hide some but not all of the changes that would be caused by ISO injection (e.g., Fig. 3 E and F). Despite the uncertainty in differentiating the effect of ISO injection and OPN deficiency on osteoclast number and surface, the data indicate without ambiguity that OPN is necessary for ISO-induced increases in systemic bone resorption activity.

We next compared osteoblastic activity in WT and OPN-KO mice treated with ISO. The basal level of mineral apposition rate (MAR), a parameter that reflects individual osteoblast-mediated bone formation, was similar in WT and OPN-KO mice (Fig. 3 H, J, and L, control). After ISO treatment, the MAR level in WT mice decreased significantly; this decrease was not observed in OPN-KO mice (Fig. 3 K and L). The bone formation rate was decreased by ~40% in response to ISO in WT but not in OPN-KO mice (Fig. 3 M), paralleling the decrease of MAR. Osteoblast number per bone surface and osteoblast surface per bone surface were suppressed by ISO in WT but not in OPN-KO mice (Fig. 3 N and O). These data indicate that sympathetic nervous tone requires OPN to decrease bone mass both by way of increased osteoclast activity and by decreased osteoblast activity.

OPN is necessary for sympathetic tone-associated osteoclast development in vitro. Given the stimulatory effect of ISO on osteoclast activity of WT mice, we next examined whether OPN regulates osteoclast development by the sympathetic tone. To this end, we used bone marrow cells taken from mice after injection of saline vehicle or ISO and cultured in the presence of vitamin D₃ (10 nM) and dexamethasone (100 nM). ISO treatment in vivo resulted in an increase in TRAP⁺ cells in bone marrow cultures from WT mice (Fig. 4A, gray bars, $P < 0.05$), reflecting a higher osteoclastic activity. In contrast, OPN deficiency did not statistically increase baseline osteoclast number ($P = 0.075$) but did prevent ISO-induced enhancement of osteoclast development in cultured bone marrow cells from ISO-treated mice (Fig. 4A, black bars). These data indicate that OPN directly mediates the development of osteoclasts in response to increased sympathetic activity.

OPN is necessary for sympathetic tone-induced gene expression in bone. To examine the effects of OPN deficiency on the sympathetic tone-induced changes in gene expression in bone cells in vivo, we compared mRNA from bones of mice treated with either vehicle or ISO. ISO injections increased the mRNA level of TRAP (Fig. 4B), a representative osteoclast marker, and conversely reduced the basal level of Runx2, an important transcription factor for osteoblastogenesis, in WT mice but not in

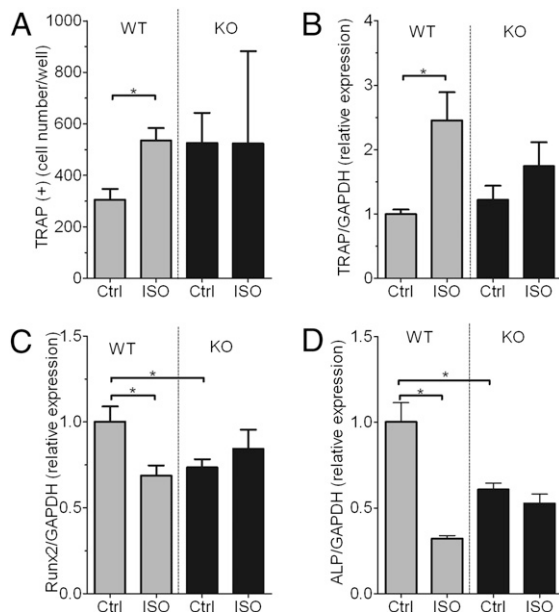


Fig. 4. OPN deficiency suppresses ISO-induced osteoclast development and changes in mRNA expression. (A) Bone marrow cells obtained from WT and OPN-KO mice treated with ISO or saline vehicle (Ctrl) were cultured in the presence of vitamin D and dexamethasone to determine osteoclast development (TRAP⁺ multinucleated cells). Bars represent the mean \pm SEM of $n = 5$ mice per group ($*P < 0.05$). (B–D) Gene expression in bone samples from WT and OPN-KO mice. Expression of TRAP (B), Runx2 (C), and alkaline phosphatase (ALP) (D), all normalized to GAPDH mRNA expression, in bone samples from WT and OPN-KO mice. Results are expressed in arbitrary units as mean \pm SEM of $n = 5$ –6 per group ($*P < 0.05$).

OPN-KO mice (Fig. 4B and C). ISO also induced suppression of alkaline phosphatase transcripts in WT mice to a significantly greater degree than in OPN-KO mice (Fig. 4D). These observations indicate that OPN is necessary for changes in the expression of genes related to bone resorption and bone formation that are induced by activation of the sympathetic tone.

Extracellular and intracellular OPN contribute to bone mass regulation by ISO. Given that OPN can act as an extracellular cytokine and as an intracellular signaling molecule (13, 14), we next used a specific and neutralizing anti-OPN monoclonal antibody (named 2C5) to differentiate the extra- and intracellular actions of OPN (13). In WT mice, treatment with 2C5 weakly attenuated (by less than 25%) the reduction of bone mass (BV/TV) induced by ISO (Fig. 5A–D). This small attenuation of ISO-induced alteration in bone architectural parameters was also observed in trabecular bone number (Fig. 5E). The effect of ISO on the enhancement of trabecular separation and trabecular spacing was also weakly attenuated by 2C5 (Fig. 5F and G). These modest attenuations contrast with the strong inhibitory effect of 2C5 in the number of osteoclasts in monolayer culture (Fig. 5H), indicating that the antibody effectively neutralized extracellular OPN. These results indicate that circulating OPN contributes only part of the protein's regulatory effect on bone metabolism.

Intracellular OPN regulates transcriptional events mediated by the β 2AR. Given that activation of β 2AR in osteoblasts contributes to bone remodeling (7), we next tested whether OPN directly regulates β 2AR signaling. We addressed this hypothesis by using several lines of experiment.

We first examined whether depletion of OPN by siRNA (as shown in Fig. S2) influences the capacity of ISO to stimulate cAMP production in MC3T3-E1 cells. To do so, we measured the time course of ISO-mediated cAMP production in individual cells with a FRET-based biosensor, epac-CFP/YFP, which has been

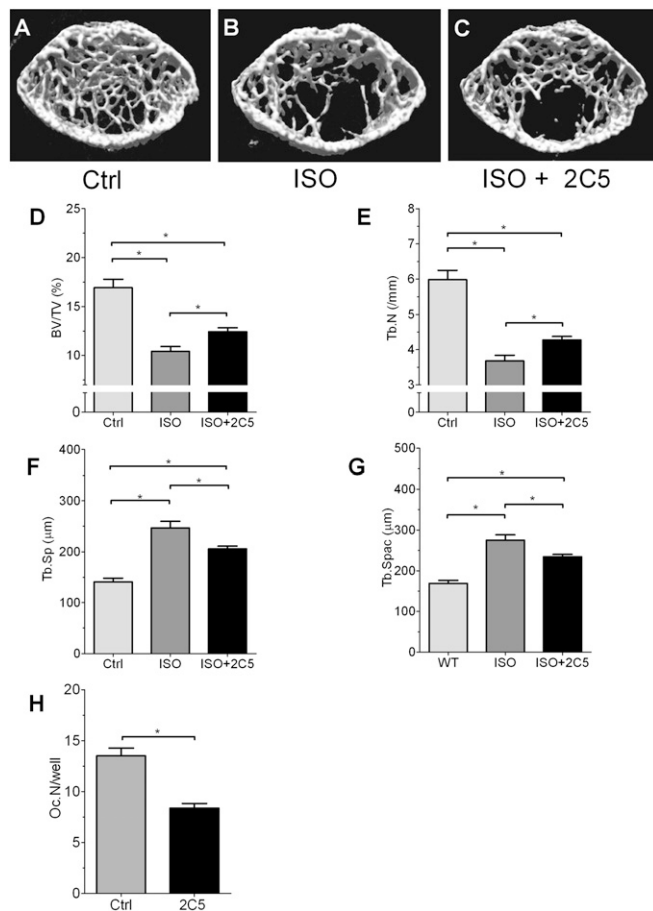


Fig. 5. Effects of neutralizing antibody against OPN on ISO-induced bone loss. (A–C) μ CT analyses of WT proximal tibiae treated with or without 2C5. (D–G) Structural parameter analysis of the tibiae. (D) BV/TV. (E) Trabecular number (Tb.N). (F) Trabecular separation (Tb.Sp). (G) Trabecular spacing (Tb.Spac). (H) In vitro reduction of osteoclast development by anti-OPN antibody, 2C5 ($*P < 0.05$).

previously described (15). In this assay, a single cell under study is continuously superfused with either control buffer or ligand. This condition thus excludes the existence of secreted extracellular OPN. Addition of ISO (10 μ M) caused a fast increase in cAMP similar to that induced by forskolin (10 μ M) (Fig. 6A). After this increase, the cAMP response was rapidly desensitized, even in the continuous presence of the ligand, consistent with previous reports (16, 17) (Fig. 6A, Left, control). The time course of cAMP generation was longer in cells depleted of OPN, and the integrated cAMP response for 30 min was significantly increased ($P < 0.01$) (Fig. 6A, si-OPN and bar graph). Conversely, overexpression of OPN (Fig. S2) reduced cAMP generation in response to ISO (10 μ M) (Fig. 6A, Right, OPN). Blockade of secreted OPN action by exposing cells to a neutralizing OPN antibody did not affect the cAMP response to ISO (Fig. S3), thus suggesting that the effect of OPN overexpression is likely mediated by intracellular OPN. A slight but significant increase in basal cAMP was also observed in the absence of OPN expression (Fig. S4). Altogether, these data suggest that intracellular OPN does regulate cAMP production mediated by β 2AR. Given that the absence of OPN had no effect on the capacity of forskolin (10 μ M) to produce a maximal cAMP response, these data indicated that OPN modulates the time course of cAMP response by acting at the level of the receptor and/or the stimulatory G protein (G_s) rather than the adenylate cyclase effector molecule. Pull-down experiments did not indicate

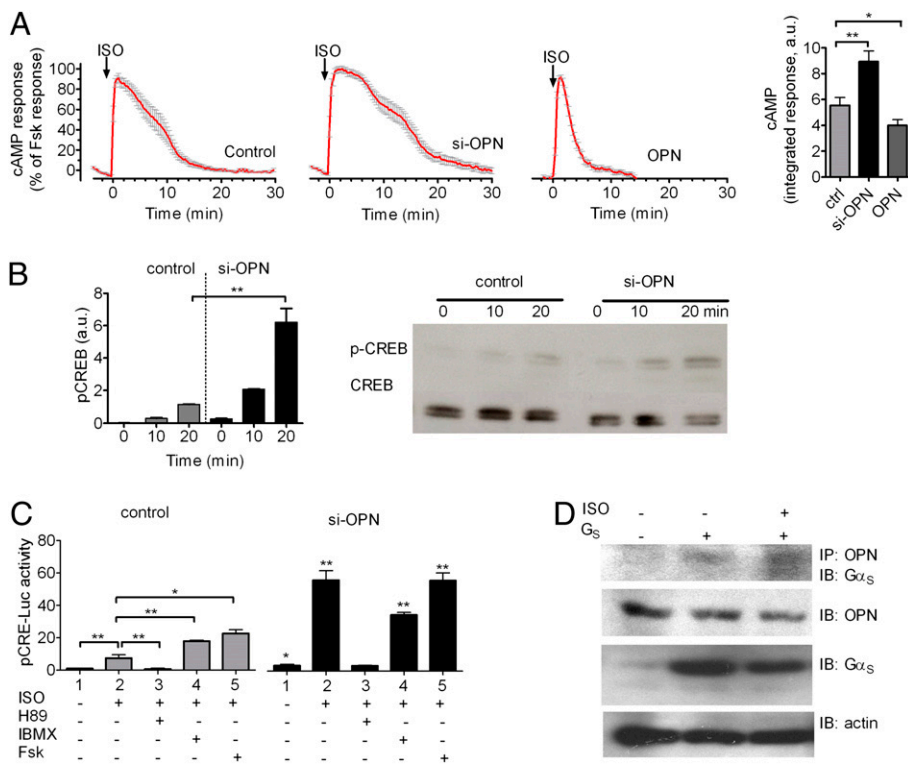


Fig. 6. OPN control of β_2 AR signaling. (A) Averaged cAMP responses mediated by ISO. cAMP induction over a 30-min time course was monitored by FRET changes from MC3T3 osteoblastic cells transiently expressing epac-CFP/YFP alone (control, *Left*) or in combination with si-OPN (*Center*) or overexpressing OPN (*Right*). Bars represent the average cAMP responses determined by measuring the area under the curve from 0 to 30 min for cAMP. Data represent the mean \pm SEM of $n = 15$ (ctrl), $n = 28$ (si-OPN), and $n = 34$ (OPN). ($*P < 0.01$, $**P < 0.05$). (B) Western blot analyses of CREB phosphorylation in control and OPN-depleted MC3T3 cells in response to 10 μ M ISO. Bars represent the mean \pm SEM of $n = 3$ ($**P < 0.01$). (C) CRE-Luc activity (pCRE-Luc) in control cells (control) and cells transfected with si-OPN in response to 10 μ M ISO with or without H89, IBMX, or forskolin (Fsk). siRNA for OPN enhanced the ISO-induced increase in the levels of luciferase activity, and H89, a PKA inhibitor, suppressed the enhancement. Bars represent the mean \pm SEM of $n = 4$ ($*P < 0.05$, $**P < 0.01$). (D) Coimmunoprecipitation of G_{α_s} and OPN. Cells transfected with G_{α_s} in combination with $G\beta_1\gamma_2$ (G_s) and empty vector were challenged with carrier or with 10 μ M ISO. OPN was immunoprecipitated with Sepharose beads conjugated with anti-C25 monoclonal antibody, and G_{α_s} was detected with a polyclonal antibody against GFP ($n = 4$). IP, immunoprecipitation; IB, immunoblot detection.

association between OPN and the receptor but rather supported the existence of transient complexes of OPN and G_{α_s} (Fig. 6D). However, detection of this complex required the use of a membrane-permeant cross-linker, dithiobis(succinimidyl) propionate, indicating a transient and potentially weak interaction. A low baseline interaction was detected when OPN and G_s were coexpressed, possibly reflecting constitutive interaction of a small fraction of OPN. Altogether, these data support a physical proximity of OPN to G_s inside the cell and suggest a role for intracellular OPN in regulating cAMP production mediated by the β_2 AR/ G_s system.

We next tested whether OPN influences the downstream signaling of β_2 AR. To do so, we measured β_2 AR-mediated phosphorylation of a cAMP-dependent transcription factor called cAMP-response element binding (CREB) protein as well as transcription of genes controlled by the CRE regulatory element in MC3T3-E1 cells. ISO stimulated CREB protein phosphorylation to a moderate degree in control cells and to a significantly greater degree in cells depleted of OPN (Fig. 6B). This enhanced capacity of ISO to stimulate CREB activity in the absence of OPN correlates with the effect of OPN on cAMP generation in the same cells (Fig. S5, *Left*). Similarly, depletion of OPN increased the changes in CRE-dependent gene expression as measured by a luciferase-based CRE reporter (CRE-Luc) (Fig. S5). Consistent with the involvement of the cAMP/PKA signaling pathway in the transcriptional regulation induced by ISO, no enhancement of ISO-induced luciferase activity was observed when OPN-specific siRNA transfected (si-OPN) cells were pretreated with H89, a specific PKA inhibitor (Fig. 6C, black bars, lane 2 vs. 3). Isobutylmethylxanthine (IBMX), an inhibitor of cAMP-specific phosphodiesterases, increased ISO-induced luciferase activity (Fig. 6C, gray bars, lane 2 vs. 4), and depletion of OPN increased luciferase activity still further (Fig. 6C, gray bar in lane 4 vs. black bar in lane 4). Forskolin, a direct activator of adenylate cyclases, had a similar effect (Fig. 6C, gray bar in lane 5 vs. black bar in lane 5). We further confirmed a role for OPN in regulating downstream signaling by β_2 AR in a mesenchymal cell line (C2C12; Fig. S6, lane

2 vs. lane 4). OPN thus inhibits CRE transcription in at least two different osteoblastic lineage cells. Interestingly, si-OPN alone slightly enhanced CRE-Luc activity in the absence of ISO in osteoblasts, similar to the increased baseline cAMP levels described above (Fig. 6C, gray bar in lane 1 vs. black bar in lane 1). Altogether, these data show that OPN inhibits both immediate and downstream signaling by β_2 AR and that OPN acts by interacting with G_s rather than with the receptor itself.

Discussion

Genetic studies have shown that the sympathetic nervous system controls bone mass by regulating local bone remodeling (7, 8). However, mechanisms that link the nervous system and bone metabolism remain poorly understood. Based on results obtained with genetic, physiological, and cell-based assays, we propose that OPN plays a key role in linking the sympathetic tone and the

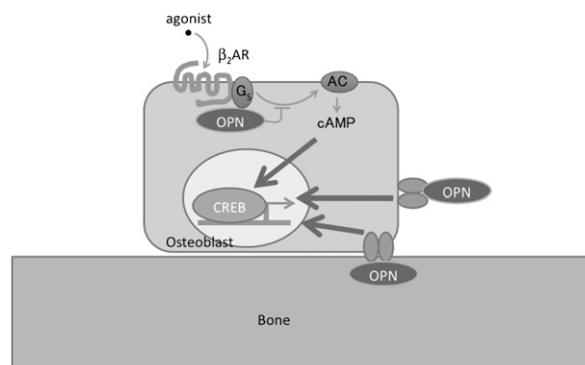


Fig. 7. Model of regulation of β_2 AR signaling by OPN. Our data suggest that intracellular OPN regulates β_2 AR signaling in osteoblasts by interacting with G_s to reduce the time course of cAMP production and CRE-dependent transcription activity to ultimately reduce bone mass. Extracellular OPN is also involved in regulation of bone cells by activation of CD44/integrin family of receptors.

regulation of bone loss by regulation of cAMP signaling by the β 2AR. First, sympathetic tone enhances OPN mRNA and protein levels in circulation and bone cells. Second, OPN is required for influence of the sympathetic tone on two aspects of bone metabolism, increased catabolic activity by osteoclasts and reduced anabolic activity by osteoclasts, resulting in decreased in bone mass. Third, OPN depletion enhances the capacity of β 2AR agonists to stimulate cAMP production, CREB protein phosphorylation, and CRE-dependent luciferase activity in cultured mouse osteoblasts, whereas OPN overexpression has the inverse effect. It is notable that loss of OPN slightly increased basal cAMP as well as CRE-Luc activity even in the absence of agonist treatment. This observation would suggest that OPN reduces both ligand-dependent and -independent signaling by β 2AR. The influence of OPN on bone metabolism is therefore at least partially attributable to direct regulation of β 2AR signaling at the cellular level. These characteristics would make OPN a key player in the regulation of bone mass by the sympathetic tone. Given that OPN has an inhibitory effect on adrenergic receptors, the up-regulation of OPN expression in bone by the sympathetic tone could represent a unique feedback pathway to influence metabolic responses not only to agonists of the β 2AR but also to other receptors.

Secreted OPN acts as a cytokine by binding extracellular domains of cell-surface receptors such as CD44 and $\alpha\beta_3$ (18). Recent reports indicate that OPN is also present in the intracellular compartment, where it can act as a signaling molecule or a scaffold (13, 19, 20). With a perfusion system and a FRET-based cAMP assay, we were able to assess the action of OPN inside the cell. Given that OPN function is also detected inside the cell, it is therefore possible that intracellular as well as secreted OPN regulate ISO-induced cAMP signaling (Fig. 7). Thus, we have identified a functional interaction between the β 2AR/ G_s system and OPN that might modulate bone mass.

Materials and Methods

Animals. OPN-deficient male mice were produced as described (12). The original chimeric mice were backcrossed with 129 S1 mice to generate 129 mixed-background mice. Animals were backcrossed to the 129 strain to obtain isogenic mice. β 2AR-deficient mice in the C57BL/6 background were produced as described (21). All animals were housed under controlled conditions at 25 °C on a 12-h light/12-h dark cycle. Experiments were approved by the animal welfare committee of the Tokyo Medical and Dental University. Mice were killed by overdose of pentobarbital.

1. Kanis JA, et al. (2003) The components of excess mortality after hip fracture. *Bone* 32: 468–473.
2. Lanyon L, Skerry T (2001) Postmenopausal osteoporosis as a failure of bone's adaptation to functional loading: a hypothesis. *J Bone Miner Res* 16:1937–1947.
3. Ehrlich PJ, Lanyon LE (2002) Mechanical strain and bone cell function: a review. *Osteoporos Int* 13:688–700.
4. Noda M, ed (2011) *Mechanosensing Biology* (Springer, Tokyo).
5. Raisz LG (2005) Pathogenesis of osteoporosis: concepts, conflicts, and prospects. *J Clin Invest* 115:3318–3325.
6. Karsenty G (2006) Convergence between bone and energy homeostases: leptin regulation of bone mass. *Cell Metab* 4:341–348.
7. Elefteriou F (2008) Regulation of bone remodeling by the central and peripheral nervous system. *Arch Biochem Biophys* 473:231–236.
8. Kondo H, et al. (2005) Unloading induces osteoblastic cell suppression and osteoclastic cell activation to lead to bone loss via sympathetic nervous system. *J Biol Chem* 280: 30192–30200.
9. Denhardt DT, Noda M, O'Regan AW, Pavlin D, Berman JS (2001) Osteopontin as a means to cope with environmental insults: regulation of inflammation, tissue remodeling, and cell survival. *J Clin Invest* 107:1055–1061.
10. Ishijima M, et al. (2001) Enhancement of osteoclastic bone resorption and suppression of osteoblastic bone formation in response to reduced mechanical stress do not occur in the absence of osteopontin. *J Exp Med* 193:399–404.
11. Ishijima M, et al. (2002) Resistance to unloading-induced three-dimensional bone loss in osteopontin-deficient mice. *J Bone Miner Res* 17:661–667.

FRET-Based cAMP Assay in Live Cells. This assay was performed with individual cells as previously described (22). In brief, cells plated on glass coverslips coated with poly-D-lysine and maintained in FRET buffer were placed on a Nikon Ti-E or Zeiss Axiovert 200 inverted microscope equipped with an oil-immersion 60 N.A. 1.49 plan-apo objective and a dichroic beam splitter to allow simultaneous recording of CFP and YFP fluorescence channels (DualView2; Photometrics or TILL Photonics). The emission fluorescence intensities were determined at 535 ± 15 nm (YFP) and 480 ± 20 nm (CFP) with a beam splitter DCLP of 505 nm. The FRET ratio for single experiments was corrected according to Eq. 1:

$$\text{Ratio} \left(\frac{F_{\text{YFP}}}{F_{\text{CFP}}} \right) = \frac{F_{\text{YFP}}^{\text{ex436/em535}} - a \times F_{\text{CFP}}^{\text{ex436/em480}} - b \times F_{\text{YFP}}^{\text{ex500/em535}}}{F_{\text{CFP}}^{\text{ex436/em480}}} \quad [1]$$

where $F_{\text{YFP}}^{\text{ex436/em535}}$ and $F_{\text{CFP}}^{\text{ex436/em480}}$ represent, respectively, the emission intensities of YFP (recorded at 535 nm) and CFP (recorded at 480 nm) upon excitation at 436 nm; a and b represent correction factors for the bleed-through of CFP into the 535-nm channel ($a = 0.35$) and the cross-talk attributable to the direct YFP excitation by light at 436 nm ($b = 0.06$). $F_{\text{YFP}}^{\text{ex500/em535}}$ represents the emission intensity of YFP (recorded at 535 nm) upon direct excitation at 500 nm and was recorded at the beginning of each experiment. Note that bleed-through of YFP into the 480-nm channel was negligible. For each measurement, changes in fluorescence emissions attributable to photobleaching were subtracted. To ensure that CFP- and YFP-labeled molecule expression were similar in examined cells, we performed experiments in cells displaying comparable fluorescence levels.

The means of FRET experiments were calculated according to Eq. 2, which normalizes for different expression levels of CFP and YFP molecules:

$$N_{\text{FRET}} = \frac{F_{\text{YFP}}^{\text{ex436/em535}} - a \times F_{\text{CFP}}^{\text{ex436/em480}} - b \times F_{\text{YFP}}^{\text{ex500/em535}}}{\sqrt{F_{\text{CFP}}^{\text{ex436/em480}} \times F_{\text{YFP}}^{\text{ex500/em535}}}} \quad [2]$$

Note that, in the epac-CFP/YFP, the $F_{\text{CFP}}/F_{\text{YFP}}$ ratio decreases upon generation of cAMP, but it is represented as a positive signal for convenience.

More details are included in *SI Materials and Methods*.

Statistical Evaluation. Data are expressed as mean \pm SEM for all values. Statistical significance of the differences was evaluated based on Student's t test or two-way ANOVA.

ACKNOWLEDGMENTS. This work was supported by Grants-in-Aid 18109011, 18659438, 18123456, and 20013014 from the Japanese Ministry of Education (Global Center of Excellence Program, International Research Center for Molecular Science in Tooth and Bone Diseases), grants from the Japan Space Forum (to M. Noda), and National Institutes of Health Award R01DK087688 (to J.-P.V.).

12. Rittling SR, et al. (1998) Mice lacking osteopontin show normal development and bone structure but display altered osteoclast formation in vitro. *J Bone Miner Res* 13:1101–1111.
13. Shinohara ML, Kim JH, Garcia VA, Cantor H (2008) Engagement of the type I interferon receptor on dendritic cells inhibits T helper 17 cell development: role of intracellular osteopontin. *Immunity* 29:68–78.
14. Cantor H, Shinohara ML (2009) Regulation of T-helper-cell lineage development by osteopontin: the inside story. *Nat Rev Immunol* 9:137–141.
15. Nikolaev VO, Bünemann M, Hein L, Hannawacker A, Lohse MJ (2004) Novel single chain cAMP sensors for receptor-induced signal propagation. *J Biol Chem* 279:37215–37218.
16. Violin JD, et al. (2008) β 2-adrenergic receptor signaling and desensitization elucidated by quantitative modeling of real time cAMP dynamics. *J Biol Chem* 283:2949–2961.
17. Feinstein TN, et al. (2011) Retromer terminates the generation of cAMP by internalized PTH receptors. *Nat Chem Biol* 7:278–284.
18. Wang KX, Denhardt DT (2008) Osteopontin: role in immune regulation and stress responses. *Cytokine Growth Factor Rev* 19:333–345.
19. Diao H, et al. (2004) Osteopontin as a mediator of NKT cell function in T cell-mediated liver diseases. *Immunity* 21:539–550.
20. Shinohara ML, Kim HJ, Kim JH, Garcia VA, Cantor H (2008) Alternative translation of osteopontin generates intracellular and secreted isoforms that mediate distinct biological activities in dendritic cells. *Proc Natl Acad Sci USA* 105:7235–7239.
21. Chruscinski AJ, et al. (1999) Targeted disruption of the β 2 adrenergic receptor gene. *J Biol Chem* 274:16694–16700.
22. Ferrandon S, et al. (2009) Sustained cyclic AMP production by parathyroid hormone receptor endocytosis. *Nat Chem Biol* 5:734–742.